British Journal of Pharmacology

DOI:10.1111/j.1476-5381.2011.01672.x
www.brjpharmacol.org

RESEARCH PAPER

Identification of drugs and drug metabolites as substrates of multidrug resistance protein 2 (MRP2) using triple-transfected MDCK-OATP1B1-UGT1A1-MRP2 cells

Correspondence
Professor Martin F. Fromm, Institute of Experimental and Clinical Pharmacology and Toxicology, Friedrich-Alexander-Universität Erlangen-Nürnberg, Emil Fischer Center, Fahrstraße 17, 91054 Erlangen, Germany.
E-mail: martin.fromm@pharmakologie.med.uni-erlangen.de

Keywords
drug transport; drug metabolism; OATP1B1; UGT1A1; MRP2; ezetimibe; etoposide; triple-transfected cells; MDCK

Received
6 May 2011
Revised
20 July 2011
Accepted
21 August 2011

C Fahrmayr, J König, D Auge, M Mieth and MF Fromm

Institute of Experimental and Clinical Pharmacology and Toxicology, Friedrich-Alexander-Universität Erlangen-Nürnberg, Erlangen, Germany

BACKGROUND AND PURPOSE

The coordinate activity of hepatic uptake transporters [e.g. organic anion transporting polypeptide 1B1 (OATP1B1)], drug-metabolizing enzymes [e.g. UDP-glucuronosyltransferase 1A1 (UGT1A1)] and efflux pumps (e.g. MRP2) is a crucial determinant of drug disposition. However, limited data are available on transport of drugs (e.g. ezetimibe, etoposide) and their glucuronidated metabolites by human MRP2 in intact cell systems.

EXPERIMENTAL APPROACH

Using monolayers of newly established triple-transfected MDCK-OATP1B1-UGT1A1-MRP2 cells as well as MDCK control cells, single- (OATP1B1) and double-transfected (OATP1B1-UGT1A1, OATP1B1-MRP2) MDCK cells, we therefore studied intracellular concentrations and transcellular transport after administration of ezetimibe or etoposide to the basal compartment.

KEY RESULTS

Intracellular accumulation of ezetimibe was significantly lower in MDCK-OATP1B1-UGT1A1-MRP2 triple-transfected cells compared with all other cell lines. Considerably higher amounts of ezetimibe glucuronide were found in the apical compartment of MDCK-OATP1B1-UGT1A1-MRP2 monolayers compared with all other cell lines. Using HEK cells, etoposide was identified as a substrate of OATP1B1. Intracellular concentrations of etoposide equivalents (i.e. parent compound plus metabolites) were affected only to a minor extent by the absence or presence of OATP1B1/UGT1A1/MRP2. In contrast, apical accumulation of etoposide equivalents was significantly higher in monolayers of both cell lines expressing MRP2 (MDCK-OATP1B1-MRP2, MDCK-OATP1B1-UGT1A1-MRP2) compared with the single-transfected (OATP1B1) and the control cell line.

CONCLUSIONS AND IMPLICATIONS

Ezetimibe glucuronide is a substrate of human MRP2. Moreover, etoposide and possibly also its glucuronide are substrates of MRP2. These data demonstrate the functional interplay between transporter-mediated uptake, phase II metabolism and export by hepatic proteins involved in drug disposition.

Abbreviations

BSP, bromosulphophthalein; MRP2, multidrug resistance protein 2; OATP1B1, organic anion transporting polypeptide 1B1; UGT1A1, UDP-glucuronosyltransferase 1A1

Introduction

Disposition and effects of a broad variety of drugs are determined by uptake transport, metabolism and efflux in the liver. Following transporter-mediated uptake into the hepatocytes [e.g. by organic anion transporting polypeptide 1B1, OATP1B1 (*SLCO1B1*)] and subsequent phase I and/or phase II metabolism [e.g. by UDP-glucuronosyltransferase 1A1, UGT1A1 (*UGT1A1*)], parent compounds and/or their metabolites are frequently exported by distinct transporters [e.g. members of the ABC transporter family such as multidrug resistance protein 2, MRP2 (*ABCC2*)] into bile (Funk, 2008; Zolk and Fromm, 2011).

The cholesterol-lowering drug ezetimibe (for structure, see Figure S1), an inhibitor of intestinal cholesterol absorption via the Niemann-Pick C1 Like 1 (NPC1L1) protein (Altmann *et al.*, 2004), undergoes extensive entero-hepatic circulation (Kosoglou *et al.*, 2005; Oswald *et al.*, 2008). Several, but not all, studies indicate that UGT1A1 is a major enzyme catalyzing glucuronidation of ezetimibe to its phenolic glucuronide [1-*O*-[4-*trans*-2*S*,3*R*)-1-(4-fluorophenyl)-4-oxo-3-[3(*S*)-hydroxy-3-(4-fluorophenyl)propyl]-2-azetidinyl]-phenyl-ß-D-glucopyranuronic acid] (Ghosal *et al.*, 2004; Cai *et al.*, 2010; Oswald *et al.*, 2011). Ezetimibe glucuronide constitutes more than 80% of ezetimibe equivalents in human plasma. UGT1A1, MRP2 and P-glycoprotein have been associated with ezetimibe disposition in humans (Oswald *et al.*, 2006a). Moreover, disposition of ezetimibe in humans is influenced by polymorphisms in the *SLCO1B1* gene encoding the hepatic uptake transporter OATP1B1 (Oswald *et al.*, 2008), localized in the basolateral membrane of human hepatocytes. Serum concentrations of ezetimibe glucuronide were considerably increased in Mrp2-deficient rats compared with wild-type animals (Oswald *et al.*, 2006a; 2010), and Mrp2-deficient mice accumulated significantly more ezetimibe glucuronide in the liver and eliminated significantly less ezetimibe glucuronide into bile compared with Mrp2-expressing animals (de Waart *et al.*, 2009). The ATP-dependent transport of 17β-glucuronosyl oestradiol into isolated MRP2-containing inside-out vesicles was inhibited by ezetimibe glucuronide (Oswald *et al.*, 2006a; de Waart *et al.*, 2009). However, to the best of our knowledge, there are no *in vitro* data regarding whether ezetimibe glucuronide is a substrate of human MRP2 or not.

Similar to ezetimibe, the anticancer agent etoposide (for structure, see Figure S1) is glucuronidated by UGT1A1 (Watanabe *et al.*, 2003), and data from Abcc2-deficient mice indicate that etoposide and its glucuronide are substrates of rodent Mrp2 (Lagas *et al.*, 2010). Etoposide is also transported by human MRP2 and MRP3 (Cui *et al.*, 1999; Zelcer *et al.*, 2001; Guo *et al.*, 2002; Huisman *et al.*, 2005). There are currently no data regarding whether etoposide is taken up by hepatic OATPs (OATP1B1, OATP1B3 and OATP2B1) and whether or not etoposide glucuronide is a substrate of human MRP2.

Direct identification of glucuronidated metabolites as MRP2 substrates can be very challenging for the following reasons: (i) The drug glucuronide is not generally available. (ii) Drug glucuronides poorly cross cellular membranes by passive diffusion. Therefore, the use of polarized monolayers stably expressing MRP2 in the apical membrane with administration of the glucuronide to the basal compartment can be problematic, because the glucuronide will not enter the cells. (iii) In addition, studies with inside-out oriented vesicles of cell lines stably expressing MRP2 are time consuming and challenging. We therefore generated and characterized Madin-Darby canine kidney (MDCK) cells, which stably express simultaneously the uptake transporter OATP1B1, the phase II drug-metabolizing enzyme UGT1A1 and the efflux transporter MRP2, in order to investigate in polarized monolayers of triple-transfected MDCK-OATP1B1-UGT1A1-MRP2 cells and in the control cell lines MDCK-Co, in single- (OATP1B1) and double-transfected cells (OATP1B1-UGT1A1 and OATP1B1-MRP2), whether or not frequently used drugs and/or their phase II metabolites are substrates of human MRP2.

Methods

Cloning of the human UGT1A1 cDNA

The UGT1A1 coding sequence (NM_000463.2) was cloned by a RT-PCR-based approach using liver total RNA (Multiple RNA panel from Clontech, Heidelberg, Germany) as template for the single-strand cDNA synthesis. Synthesis of single-strand cDNA was performed as described earlier (König *et al.*, 1999). Full-length *UGT1A1* cDNA was amplified using the primer pair oUGT1A1-5′.for (5′-AAA GGC GCC ATG GCT GTG GA-3′) and the reverse primer oUGT1A1-RT.rev (5′-CCC ACC CAC TTC TCA ATG GG-3′) and cloned into the pCR2.1-TOPO vector (Invitrogen GmbH, Karlsruhe, Germany). Following sequencing by AGOWA (Berlin, Germany), the verified UGT1A1 coding sequence was cloned into the expression vector pcDNA3.1/Zeo(–) (Invitrogen GmbH). Three coding base pair exchanges were corrected using the QuikChange multisite-directed mutagenesis kit (Stratagene, Amsterdam, The Netherlands). On completion of the plasmid, the correctness and the orientation of the cDNA were verified by sequencing (AGOWA).

Generation of stably transfected cells

Generation and validation of MDCK-Co, MDCK-OATP1B1 and MDCK-OATP1B1-MRP2 cell lines have been described before (Cui *et al.*, 1999; König *et al.*, 2000; Fehrenbach *et al.*, 2003). In order to generate the MDCK-OATP1B1-UGT1A1 double-transfected and MDCK-OATP1B1-UGT1A1-MRP2 triple-transfected cell line, MDCK-OATP1B1 and MDCK-OATP1B1-MRP2 cells were transfected with the plasmid pcDNA3.1/Zeo(–)-UGT1A1 using the Effectene transfection reagent kit according to the manufacturer's instructions (QIAGEN GmbH, Hilden, Germany), respectively. After additional selection with zeocin (500 $\mu g \cdot mL^{-1}$), single colonies of both transfectants were screened for *UGT1A1* mRNA expression using RT-PCR and LightCycler-based quantitative RT-PCR (Roche Diagnostics-Applied Science, Mannheim, Germany), as described previously (Mandery *et al.*, 2009), to detect the cell clones with the highest expression. For comparative expression analysis, the cell clones of both newly established transfectants exhibiting the highest expression of UGT1A1 as well as the control cell lines MDCK-Co, MDCK-OATP1B1 and MDCK-OATP1B1-MRP2 were then tested for

Table 1
Sequences of primers used for quantitative real-time PCR

	Forward primer	Reverse primer	Fragment length (bp)
OATP1B1	5′-TGC ACT TGG AGG CAC CTC AC-3′	5′-CTT CAT CCA TGA CAC TTC CAT TT-3′	359
UGT1A1	5′-GTT ACA AGG AGA ACA TCA TG-3′	5′-CCC ACC CAC TTC TCA ATG GG-3′	310
MRP2	5′-CTT CGG AAA TCC AAG ATC CTG G-3′	5′-TAG AAT TTT GTG CTG TTC ACA TTC T-3′	284
ß-actin	5′-TGA CGG GGT CAC CCA CAC TGT GCC CAT CTA-3′	5′-CTA GAA GCA TTT GCG GTG GAC GAT GGA GGG-3′	661

their *SLCO1B1* mRNA (encoding OATP1B1), *UGT1A1* mRNA (encoding UGT1A1) and *ABCC2* mRNA (encoding MRP2) expression as well. All expression values were normalized to the housekeeping gene *β-actin*. Primers used for quantitative real-time PCR are listed in Table 1. The cell clones with the highest *UGT1A1* mRNA expression and a *SLCO1B1* and/or *ABCC2* mRNA expression comparable with the expression of the control cell lines (MDCK-OATP1B1 and MDCK-OATP1B1-MRP2) were chosen for further experiments.

Immunoblot analysis

Immunoblot analysis was performed as described previously (Seithel *et al.*, 2007; Mandery *et al.*, 2009). For detection of OATP1B1, UGT1A1 and MRP2, 5 µg of total homogenates of all cell lines were diluted with Laemmli buffer (62 mM Tris–HCl, 2% SDS, 10% glycerol, 0.01% bromphenol blue and 0.4 mM dithiothreitol) and incubated for 5 min at 95°C [except for MRP2 samples (Mandery *et al.*, 2009)] before separation on 7.5% (for MRP2) and 10% (for OATP1B1 and UGT1A1) SDS-polyacrylamide gels. Afterwards, the separated proteins were transferred onto a nitrocellulose membrane (PROTRAN, Whatman Schleicher and Schuell, Dassel, Germany) and incubated with a purified rabbit polyclonal anti-human OATP1B1 antiserum [pESL; 1:500; (König *et al.*, 2000)], with a rabbit polyclonal anti-human UGT1A1 antibody (ab62600; 1:400; Abcam, Cambridge, UK) and with a rabbit polyclonal anti-human MRP2 antibody [EAG5; 1:5000; kindly provided by Professor Dr Dietrich Keppler; DKFZ, Heidelberg, Germany; (Keppler and Kartenbeck, 1996; Jedlitschky *et al.*, 1997)]. As secondary antibody, a horseradish peroxidase-conjugated goat anti-rabbit IgG from Amersham (GE Healthcare UK Ltd., Little Chalfont, Buckinghamshire, UK) was used at a 1:10 000 dilution (Seithel *et al.*, 2007). Protein bands were visualized with the ChemiDoc XRS imaging system (Biorad, Munich, Germany) using ECL Western blotting detection reagents (GE Healthcare UK Ltd.). Subsequently, the membranes were stripped and re-incubated with a mouse monoclonal anti-human β-actin antibody (1:10 000; Sigma-Aldrich Chemie GmbH, Taufkirchen, Germany) and detected as described above. As a positive control, different amounts of total homogenates of the MDCK-OATP1B1-UGT1A1-MRP2 triple-transfected cell line were used to calculate a regression curve, and blots were analysed using the Quantity One Software (Biorad). The assays for all proteins were linear over the entire concentration range.

Uptake and vectorial transport assays

Uptake experiments using HEK293 cells were performed as described previously (Mandery *et al.*, 2009; Kindla *et al.*, 2011). In brief, HEK293 cells stably expressing the uptake transporters OATP1B1, OATP2B1 or OATP1B3 and the respective control cell lines (control cell lines transfected with the empty expression vectors pcDNA3.1(+) and pcDNA3.1/Hygro) were seeded at an initial density of 7×10^5 cells per well in 12-well-plates coated with poly-D-lysine and grown for 2 days. Twenty-four hours before the uptake experiments, cells were treated with 10 mM sodium butyrate (Merck KGaA, Darmstadt, Germany) to increase protein expression (Cui *et al.*, 1999). After being washed with pre-warmed (37°C) uptake buffer (142 mM NaCl, 5 mM KCl, 1 mM K_2HPO_4, 1.2 mM $MgSO_4$, 1.5 mM $CaCl_2$, 5 mM glucose and 12.5 mM HEPES, pH 7.3), cells were incubated with a mixture of radiolabelled and unlabelled etoposide at 37°C for 5 min. For the determination of the K_m value, concentrations ranging from 0.1 to 100 µM etoposide were used. Uptake of etoposide was stopped by washing three times with ice-cold uptake buffer. Subsequently, cells were lysed with 0.2% SDS, and an aliquot was used to determine the intracellular accumulation of radioactivity by liquid scintillation counting (TriCarb 2800; PerkinElmer, Boston, MA, USA). The respective protein concentration of each well was determined by bicinchonic acid assay (BCA Protein Assay Kit).

Vectorial transport assays with [^{3}H] ezetimibe and [^{3}H] etoposide were investigated in transfected MDCK cells as described previously (Cui *et al.*, 2001; Fehrenbach *et al.*, 2003) and conducted in general as described for uptake experiments with the following exceptions. MDCK cells were seeded onto ThinCerts (diameter 14 mm; pore size 0.4 µm; Greiner Bio-One GmbH, Frickenhausen, Germany) at an initial density of 4×10^5 cells per well and grown for 3 days. Twenty-four hours before transport experiments, the cells were induced with 10 mM sodium butyrate. Radiolabelled ezetimibe or etoposide were dissolved in uptake buffer, and unlabelled ezetimibe

or etoposide were added to a final concentration of 1 and 10 μM respectively. After being washed with pre-warmed uptake buffer, cells were incubated with 800 μL uptake buffer in the apical compartment and 800 μL uptake buffer containing ezetimibe or etoposide in the basolateral compartment for 30 min (ezetimibe), 60 and 120 min (etoposide) at 37°C. At the indicated time points, aliquots from the apical compartments were taken for the determination of the radioactivity in the apical compartment by liquid scintillation counting. Subsequently, cells were washed three times with ice-cold uptake buffer, filters were detached from the chambers and intracellular accumulation of radioactivity was measured after lysing the cells with 0.2% SDS. Protein concentrations of the cell lysates were determined by bicinchonic acid assay. For experiments with unlabelled ezetimibe, vectorial transport assays were performed as described above, and the amounts of ezetimibe and ezetimibe glucuronide were determined by a LC/MS/MS method using an API 4000 mass spectrometer (Applied Biosystems, Darmstadt, Germany).

Additionally, as a positive control, intracellular accumulation of the prototypical substrate bromosulphophthalein (BSP; 0.05 μM; 30 min) was determined in MDCK cells stably expressing the uptake transporter OATP1B1 in comparison to the control cell line (Cui *et al.*, 2001). Transcellular leakage was investigated by incubating the cells with 50 μM [^{3}H] inulin in the basolateral compartments for 60 and 120 min and determination of the radioactivity appearing in the apical compartment.

Quantification of ezetimibe and its glucuronide by LC/MS/MS

Unchanged ezetimibe and ezetimibe glucuronide were quantified in SDS-cell lysate and uptake buffer with slight modifications according to a method published by Oswald *et al.* (2006b). In brief, 150 μL SDS-cell lysate or buffer was diluted in deionized water, and 4-hydroxychalcon in acetonitrile was added as internal standard. The samples were extracted by means of methyl tert-butyl ether. After centrifugation, a fraction of the organic layer was separated and evaporated. The residue was dissolved in mobile phase and directly used for chromatography. For the determination of total ezetimibe (unchanged ezetimibe plus ezetimibe glucuronide), β-glucuronidase, which was diluted in water, was added to the samples. The samples were incubated at 50°C for 60 min and cooled down to room temperature. Then the internal standard was added, and the sample was extracted as described above. LC/MS/MS analysis was performed applying electrospray ionization (ESI) in the negative ion mode because we expected less matrix effects in lysate and buffer than in other biological fluids.

An API 4000 mass spectrometer (Applied Biosystems) equipped with an Agilent 1100 HPLC System (Agilent Technologies, Waldbronn, Germany) was used. Data were acquired with Analyst 1.4.2 software (Applied Biosystems). Chromatography was carried out isocratically using a mixture of acetonitrile/water (60/40, v/v) with 0.2% acetic acid as mobile phase at a flow rate of 0.4 mL·min^{-1}. A Nucleosil 100-5 C18 AB column (125 mm × 2 mm, particle size 5 μm, Macherey Nagel, Düren, Germany) with a guard column (8 mm × 3 mm, particle size 5 μm, Macherey Nagel) was used for chromatographic separation. The mass spectrometer was operating in the multiple reaction monitoring (MRM) mode. Nitrogen was used as collision (128.9 kPa), curtain (239.3 kPa), ion source one (308.2 kPa) and two (377.1 kPa) gas. Temperature of the heaters was 500°C, and the ion spray voltage was –4500 V. The mass transitions and collision energies were *m/z* 408.2 to 271.0 (–22 eV) for ezetimibe and *m/z* 223.0 to 117.0 (–22 eV) for 4-hydroxychalcon. The validated calibration range was between 1 and 1000 ng·mL^{-1}. The lower limit of quantification was 1 ng·mL^{-1}. Intra-day coefficients of variation ranged from 1.47% to 5.93% for ezetimibe and from 4.06% to 8.50% for incubated ezetimibe. The intra-day accuracies ranged from –8.46 to –0.88 for ezetimibe and from 0.46 to 2.48 for incubated ezetimibe. Inter-assay variability and matrix (lysate, buffer, β-glucuronidase/lysate and β-glucuronidase/buffer) effects were investigated by comparison of four calibration curves (1–100 ng·mL^{-1}) prepared each on a different day. The coefficients of variation varied between 2.29% and 10.54%, and accuracies varied between –3.69 and 1.98.

Data and statistical analysis

Intracellular and apical accumulation of ezetimibe glucuronide, using unlabelled ezetimibe as substrate, was determined by subtracting the amount of free ezetimibe from the amount of total ezetimibe (free ezetimibe and ezetimibe glucuronide) that could be measured in the same sample by LC/MS/MS after treatment with β-glucuronidase. Each concentration and time point was investigated at least on two separate days with at least three wells per day (i.e. $n = 6$ or higher). Real-time PCR and immunoblot analysis determining mRNA and protein expression were repeated three times. All data are presented as mean ± SD. Multiple comparisons were analysed by ANOVA with subsequent Tukey–Kramer multiple comparison test by using Prism 3.01 (GraphPad Software, San Diego, CA). Pairwise comparisons were calculated by unpaired *t*-tests. A value of $P < 0.05$ was required for statistical significance.

Materials

[^{3}H] Ezetimibe (45 Ci·mmol^{-1}) and [^{3}H] etoposide (20 Ci·mmol^{-1}) were obtained from American Radiolabeled Chemicals (St. Louis, MO). [^{3}H] Inulin (2.25 Ci·mmol^{-1}) was from PerkinElmer, and [^{3}H]-BSP (14 Ci·mmol^{-1}) was from Hartmann Analytic (Braunschweig, Germany). Unlabelled ezetimibe and etoposide were purchased from Biotrend GmbH (Wangen, Switzerland). Unlabelled BSP and inulin, poly-D-lysine hydrobromide, β-glucuronidase (≥100 000 Fishman units·mL^{-1}) and 4-hydroxychalcon were obtained from Sigma-Aldrich Chemie GmbH. Water-Baker analysed LC/MS-reagent was from Mallinckrodt Baker B.V. (Deventer, The Netherlands). Sodium butyrate, tert-butyl methyl ether for HPLC and acetonitrile hypergrade for LC/MS were purchased from Merck KGaA. The selection antibiotics zeocin, G418 (geniticin) disulphate and hygromycin were from Invitrogen GmbH. All other chemicals and reagents, unless stated otherwise, were obtained from Carl Roth GmbH + Co.KG (Karlsruhe, Germany) and were of the highest grade available.

Results

Expression analysis of OATP1B1, UGT1A1 and MRP2 in single-, double- and triple-transfected cell lines

mRNA and protein expression of OATP1B1, UGT1A1 and MRP2 in MDCK control cells, single- (OATP1B1), double- (OATP1B1-UGT1A1, OATP1B1-MRP2) and triple-transfected cells (OATP1B1-UGT1A1-MRP2) are shown in Figures 1 and 2. All cell lines expressed only the expected mRNAs and proteins, whereas no significant amounts were detectable in the MDCK control cells.

Intracellular accumulation and vectorial transport of ezetimibe equivalents to the apical compartment of monolayers of MDCK-control, single-, double- and triple-transfected cells

For all MDCK cells, transcellular leakage was determined by administration of [^{3}H] inulin to the basolateral compartments, and the amount found in the apical compartments did not exceed 1.5% (after 60 min) and 2.5% (after 120 min) of the added radioactivity (data not shown), which is in the range of previously published data (Cui *et al.*, 2001; Kopplow *et al.*, 2005). [^{3}H]Ezetimibe was administered to the basal side of the cell monolayers of MDCK-control (Co), single- (OATP1B1), double- (OATP1B1-UGT1A1, OATP1B1-MRP2) and triple-transfected cells (OATP1B1-UGT1A1-MRP2). Intracellular accumulation of ezetimibe equivalents (i.e. parent compound and metabolites) and translocation of ezetimibe equivalents into the apical compartment are shown in Figure 3. Intracellular accumulation of ezetimibe equivalents was not significantly different between control cells and MDCK-OATP1B1 cells (Figure 3A), whereas the prototypical OATP1B1 substrate BSP accumulated significantly in MDCK-OATP1B1 cells compared with the control cells (0.05 μM BSP; MDCK-Co vs. MDCK-OATP1B1 cells at 30 min: 0.43 ± 0.02 vs. 0.75 ± 0.10 pmol·mg^{-1} protein·min^{-1}, $P < 0.01$). Intracellular accumulation of ezetimibe equivalents was significantly ($P < 0.001$) lower in the MDCK-OATP1B1-UGT1A1-MRP2 triple-transfected cells compared with all other cell lines (Figure 3A). Accordingly, considerably higher amounts of ezetimibe equivalents were found in the apical compartment of monolayers of MDCK-OATP1B1-UGT1A1-MRP2 triple-transfected cells compared with all other cell lines ($P < 0.001$, Figure 3B). Significantly higher amounts of ezetimibe equivalents were also detectable in the apical compartment of monolayers of MDCK-OATP1B1-UGT1A1 double-transfected cells compared with MDCK-control, MDCK-OATP1B1 and MDCK-OATP1B1-MRP2 cells ($P < 0.001$, Figure 3B), most likely (see also below) due to transport of ezetimibe glucuronide formed in the MDCK-OATP1B1-UGT1A1 cells by endogenous canine MRP2 (Ng *et al.*, 2003). After normalization of the amount of ezetimibe equivalents transported into the apical compartment to the respective UGT1A1 content, there was no statistical significant difference between the MDCK-OATP1B1-UGT1A1 cells and the MDCK-OATP1B1-UGT1A1-MRP2 cells.

In addition to the results shown here with 30 min incubations, uptake and vectorial transport studies were also conducted with incubation times of 60 min. The amounts of

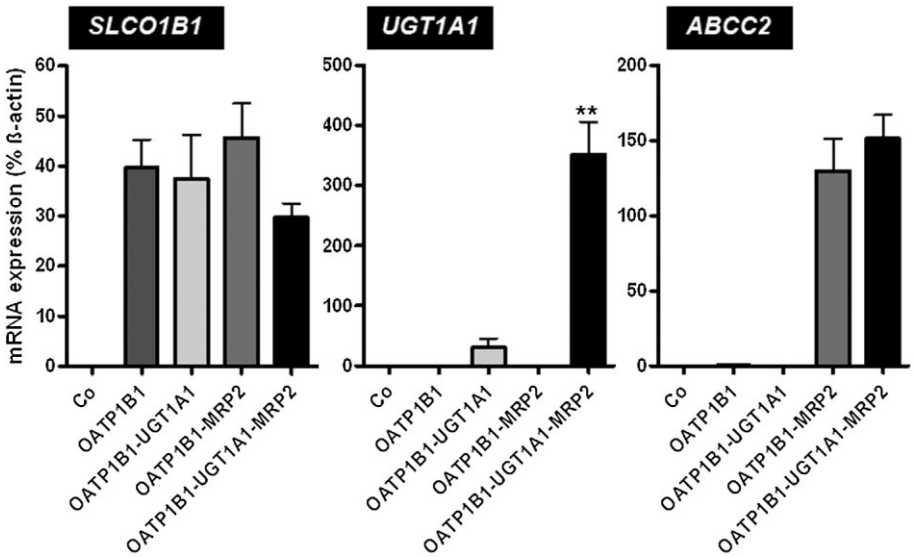

Figure 1

RT-PCR analysis of *SLCO1B1* (encoding OATP1B1), *UGT1A1* (encoding UGT1A1) and *ABCC2* (encoding MRP2) mRNA expression in MDCK control cells (Co), single- (OATP1B1), double- (OATP1B1-UGT1A1, OATP1B1-MRP2) and triple-transfected cells (OATP1B1-UGT1A1-MRP2) used in this study. Real-time PCR analysis determining mRNA expression was repeated three times. All data are presented as mean ± SD. Statistical analyses were performed between the transfected cell lines among themselves. No expression of human *SLCO1B1*, *UGT1A1* or *ABCC2* mRNA could be detected in control cells (Co). Multiple comparisons were analysed by ANOVA with subsequent Tukey–Kramer multiple comparison test. Pairwise comparisons were calculated by unpaired *t*-tests. **$P < 0.01$ versus MDCK-OATP1B1-UGT1A1 cells.

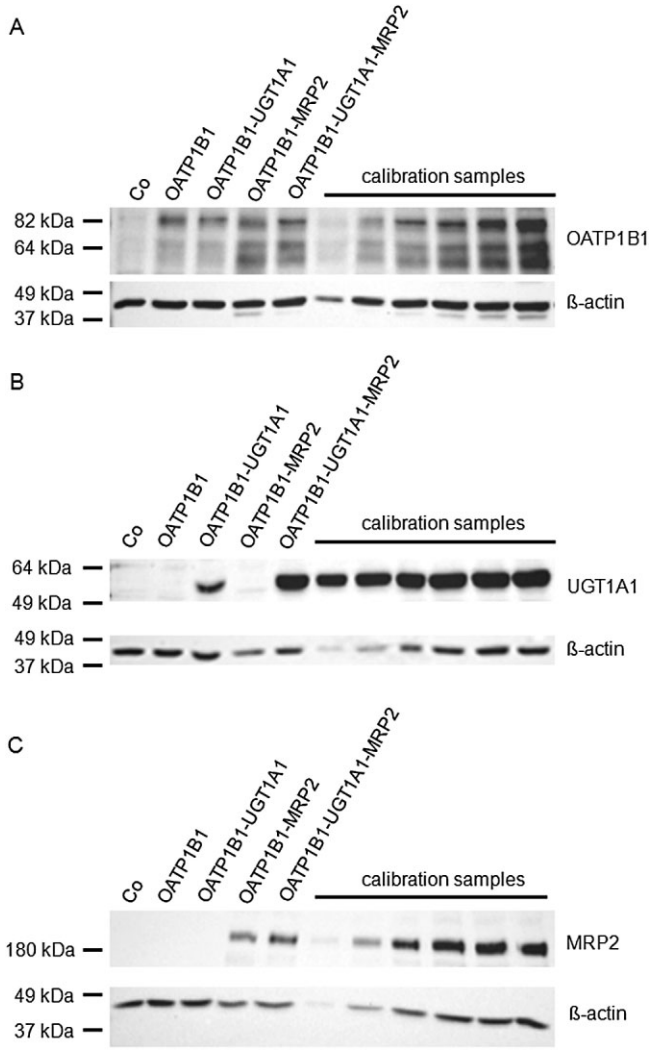

Figure 2

Immunoblot analyses of OATP1B1 (A), UGT1A1 (B) and MRP2 (C) expression in MDCK control cells (Co), single- (OATP1B1), double- (OATP1B1-UGT1A1, OATP1B1-MRP2) and triple-transfected cells (OATP1B1-UGT1A1-MRP2) used in this study. 5 µg protein of each cell line was loaded. As positive controls, calibration samples (1, 2.5, 5, 7.5, 10 and 12.5 µg protein) of the triple-transfected cell line (OATP1B1-UGT1A1-MRP2) were also loaded.

intracellular ezetimibe equivalents were very similar between the 30 and 60 min incubations, whereas the apical amount of ezetimibe equivalents approximately doubled for all cell lines (data not shown).

Intracellular accumulation and vectorial transport of ezetimibe and ezetimibe glucuronide to the apical compartment of monolayers of MDCK-control, single-, double- and triple-transfected cells

To differentiate between ezetimibe and ezetimibe glucuronide, unlabelled ezetimibe was administered to the basal side of the cell monolayers of MDCK-control (Co), single- (OATP1B1), double- (OATP1B1-UGT1A1, OATP1B1-MRP2) and triple-transfected cells (OATP1B1-UGT1A1-MRP2). Intracellular accumulation of ezetimibe and translocation of ezetimibe and ezetimibe glucuronide into the apical compartment were determined by LC/MS/MS (Figure 4). The amount of intracellular ezetimibe in the different cells was in agreement with the values found after administration of radiolabelled ezetimibe (Figures 3A and 4A), indicating that intracellular radioactivity is predominantly due to the presence of unchanged, parent compound. Intracellular accumulation of ezetimibe was significantly ($P < 0.001$) lower in the MDCK-OATP1B1-UGT1A1-MRP2 triple-transfected cells compared to all other cell lines (Figure 4A), in line with the findings shown in Figure 3A. Only modest amounts of unchanged ezetimibe reached the apical compartment (Figure 4B) with significantly lower values in the MDCK-OATP1B1-UGT1A1-MRP2 triple-transfected cells compared with all other cell lines ($P < 0.001$, Figure 4B). In line with the previous findings, considerably higher amounts of ezetimibe glucuronide were found in the apical compartment of monolayers of MDCK-OATP1B1-UGT1A1-MRP2 triple-transfected cells compared with all other cell lines ($P < 0.001$, Figure 4C). After normalization of the amount of ezetimibe glucuronide transported into the apical compartment to the differences in UGT1A1 content, there was a significant difference in the apical accumulation of ezetimibe glucuronide in monolayers of MDCK-OATP1B1-UGT1A1 cells compared with MDCK-OATP1B1-UGT1A1-MRP2 cells (232 ± 16 vs. 489 ± 28 pmol a.u.$^{-1}$, $P < 0.001$).

Identification of etoposide as substrate of OATP1B1

Uptake of [^{3}H] etoposide was investigated into HEK-OATP1B1, HEK-OATP1B3 and HEK-OATP2B1 and respective control cells. A significant uptake compared to the control cells was observed for OATP1B1 and OATP2B1 at both concentrations tested (uptake ratio OATP1B1/control 1 µM: 1.9-fold, $P < 0.0001$, 10 µM: 1.6-fold, $P = 0.0001$; uptake ratio OATP2B1/control 1 µM: 1.5-fold, $P < 0.01$, 10 µM: 1.7-fold, $P < 0.0001$; Figure 5A). HEK-OATP1B3 cells showed a modest uptake at 1 µM compared with control cells (uptake ratio OATP1B3/control 1 µM: 1.3-fold, $P < 0.05$; Figure 5A). The concentration-dependent uptake kinetics of etoposide into HEK-OATP1B1 and control cells as well as the respective net transport is shown in Figure 5B. The K_m value for OATP1B1-mediated etoposide transport was 42.2 ± 11.6 µM (Figure 5B).

Intracellular accumulation and vectorial transport of etoposide equivalents to the apical compartment of monolayers of MDCK-control, single-, double- and triple-transfected cells

[^{3}H] Etoposide was administered to the basal side of monolayers of MDCK-control, single- (OATP1B1), double- (OATP1B1-UGT1A1, OATP1B1-MRP2) and triple-transfected cells (OATP1B1-UGT1A1-MRP2). Intracellular accumulation of etoposide equivalents in the cells and translocation of etoposide equivalents into the apical compartment are shown in Figure 6. Although etoposide was clearly a substrate

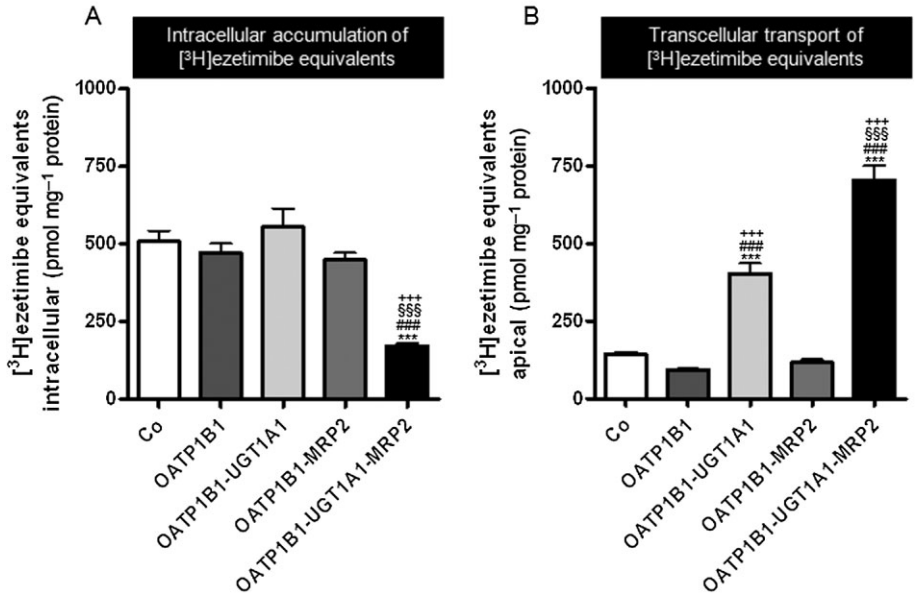

Figure 3

[^{3}H] Ezetimibe (1 μM) was administered to the basal side of monolayers of MDCK-control (Co), single- (OATP1B1), double- (OATP1B1-UGT1A1, OATP1B1-MRP2) and triple-transfected cells (OATP1B1-UGT1A1-MRP2). Intracellular accumulation of ezetimibe equivalents (i.e. parent compound and metabolites) in the cells (A) and translocation of ezetimibe equivalents into the apical compartment after 30 min (B) are shown. Data are shown as mean value ± SD. $^{***}P < 0.001$ versus MDCK-Co; $^{###}P < 0.001$ versus MDCK-OATP1B1, $^{§§§}P < 0.001$ versus MDCK-OATP1B1-UGT1A1, $^{+++}P < 0.001$ versus MDCK-OATP1B1-MRP2 cells.

of OATP1B1 (see above), the intracellular amount of etoposide equivalents was not significantly different between cells of MDCK-OATP1B1- and MDCK-control monolayers, which could be due to efflux of etoposide via canine export pumps (Ng *et al.*, 2003). The amount of etoposide equivalents accumulating over 60 and 120 min in the apical compartment was also not significantly different between MDCK-OATP1B1 and MDCK-control cells. Overall, intracellular concentrations of etoposide equivalents were affected only to a minor extent by the absence or presence of OATP1B1/UGT1A1/MRP2 (Figure 6A and B). In contrast, apical accumulation of etoposide equivalents was significantly higher in monolayers of both cell lines expressing MRP2 (MDCK-OATP1B1-MRP2, MDCK-OATP1B1-UGT1A1-MRP2) compared with the MDCK-control and the MDCK-OATP1B1 cell lines ($P < 0.01$, Figure 6D), indicating that etoposide and possibly also its glucuronide are substrates of MRP2.

Discussion and conclusions

Polarized cell lines stably transfected with uptake and efflux transporters are very useful tools in the understanding of hepatobiliary transport (see Cui *et al.*, 2001; Kopplow *et al.*, 2005; Nies *et al.*, 2008; Sato *et al.*, 2008; König *et al.*, 2010). Using a new cellular model expressing in addition to uptake and efflux transporters an additional component of hepatic drug disposition, the phase II enzyme UGT1A1, we were able to show that the pharmacologically active metabolite of the lipid-lowering drug ezetimibe, ezetimibe glucuronide, is efficiently transported by human MRP2, whereas ezetimibe, if at all, is a rather poor substrate of MRP2. Clinical studies in healthy volunteers showed that OATP1B1, UGT1A1 and MRP2 are determinants of ezetimibe disposition (Oswald *et al.*, 2006a; 2008). Previously, our own *in vitro* experiments indicated that ezetimibe and ezetimibe glucuronide are inhibitors of OATP1B1-, OATP1B3- and OATP2B1-mediated BSP transport (Oswald *et al.*, 2008). Only ezetimibe glucuronide, but not ezetimibe, was transported by OATP1B1 (Oswald *et al.*, 2008). This is in line with results from the present study, which revealed no significant differences between intracellular amounts of ezetimibe in monolayers of MDCK control cells and those in MDCK-OATP1B1 single-transfected cells.

Intracellular accumulation of ezetimibe was significantly lower in the MDCK-OATP1B1-UGT1A1-MRP2 triple-transfected cells compared with all other cell lines, which is due to glucuronidation of ezetimibe by UGT1A1 and subsequent export into the apical compartment by MRP2. Only modest amounts of unchanged ezetimibe reached the apical compartment in all cell lines with significantly lower values in the MDCK-OATP1B1-UGT1A1-MRP2 triple-transfected cells compared with all other cells, which is due to extensive phase II metabolism of ezetimibe and subsequent export by MRP2. Interestingly, after taking into account differences in UGT1A1 content, considerably higher amounts of ezetimibe glucuronide were found in the apical compartment of monolayers of MDCK-OATP1B1-UGT1A1-MRP2 triple-transfected cells compared with all other cell lines, indicating that the coordinate function of UGT1A1 and MRP2 is crucial for

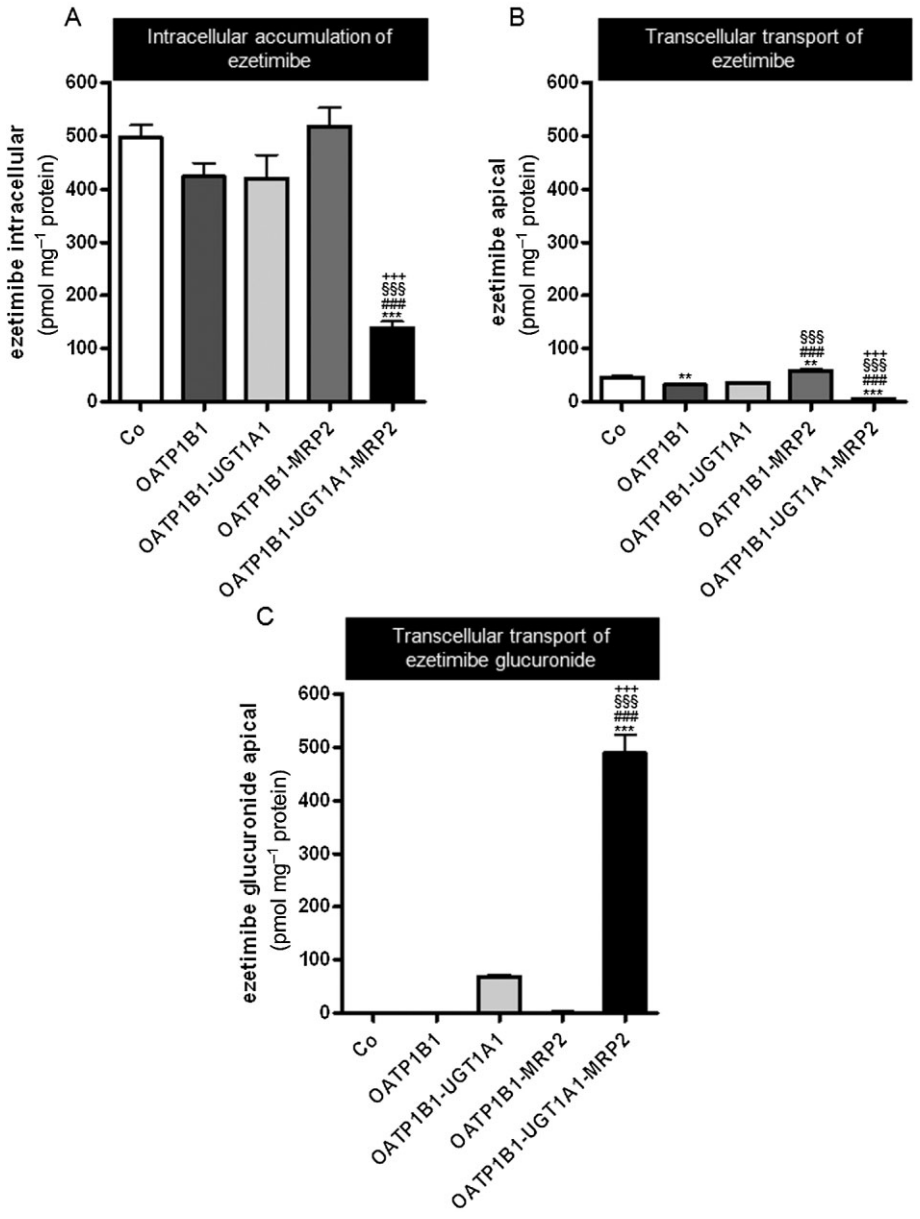

Figure 4

Unlabelled ezetimibe (1 μM) was administered to the basal side of monolayers of MDCK-control (Co), single- (OATP1B1), double- (OATP1B1-UGT1A1, OATP1B1-MRP2) and triple-transfected cells (OATP1B1-UGT1A1-MRP2). Intracellular accumulation of ezetimibe in the cells (A) and translocation of ezetimibe (B) and ezetimibe glucuronide (C) into the apical compartment after 30 min are shown. Data are shown as mean value ± SD. $^{**}P < 0.01$, $^{***}P < 0.001$ versus MDCK-Co; $^{###}P < 0.001$ versus MDCK-OATP1B1, $^{§§§}P < 0.001$ versus MDCK-OATP1B1-UGT1A1, $^{+++}P < 0.001$ versus MDCK-OATP1B1-MRP2 cells.

apical accumulation of ezetimibe glucuronide. After oral administration of [^{14}C] ezetimibe to healthy volunteers, 78% of radioactivity was recovered in faeces (Patrick *et al.*, 2002). Surprisingly, unconjugated ezetimibe was the major compound in faeces, although ezetimibe is extensively conjugated in humans, suggesting low absorption and/or hydrolysis of ezetimibe glucuronide secreted into bile (Patrick *et al.*, 2002; Kosoglou *et al.*, 2005).

Our findings on phase II metabolism of ezetimibe and export of its glucuronide by human MRP2 are in line with previous studies: Ghosal *et al.* (2004) showed that UGT1A1 together with UGT1A3 and UGT2B15 are the enzymes catalysing formation of the phenolic glucuronide conjugate of ezetimibe. It should be noted that Cai *et al.* (2010) reported recently that ezetimibe conjugation is catalysed by UGT2B proteins and possibly not to a major extent by UGT1A1. In contrast, Oswald *et al.* (2011) found *in vitro* glucuronidation of ezetimibe by UGT1A1 and UGT1A3, but not by UGT2B7 and UGT2B15. Our findings are in line with the data published by Ghosal *et al.* (2004) and Oswald *et al.* (2011),

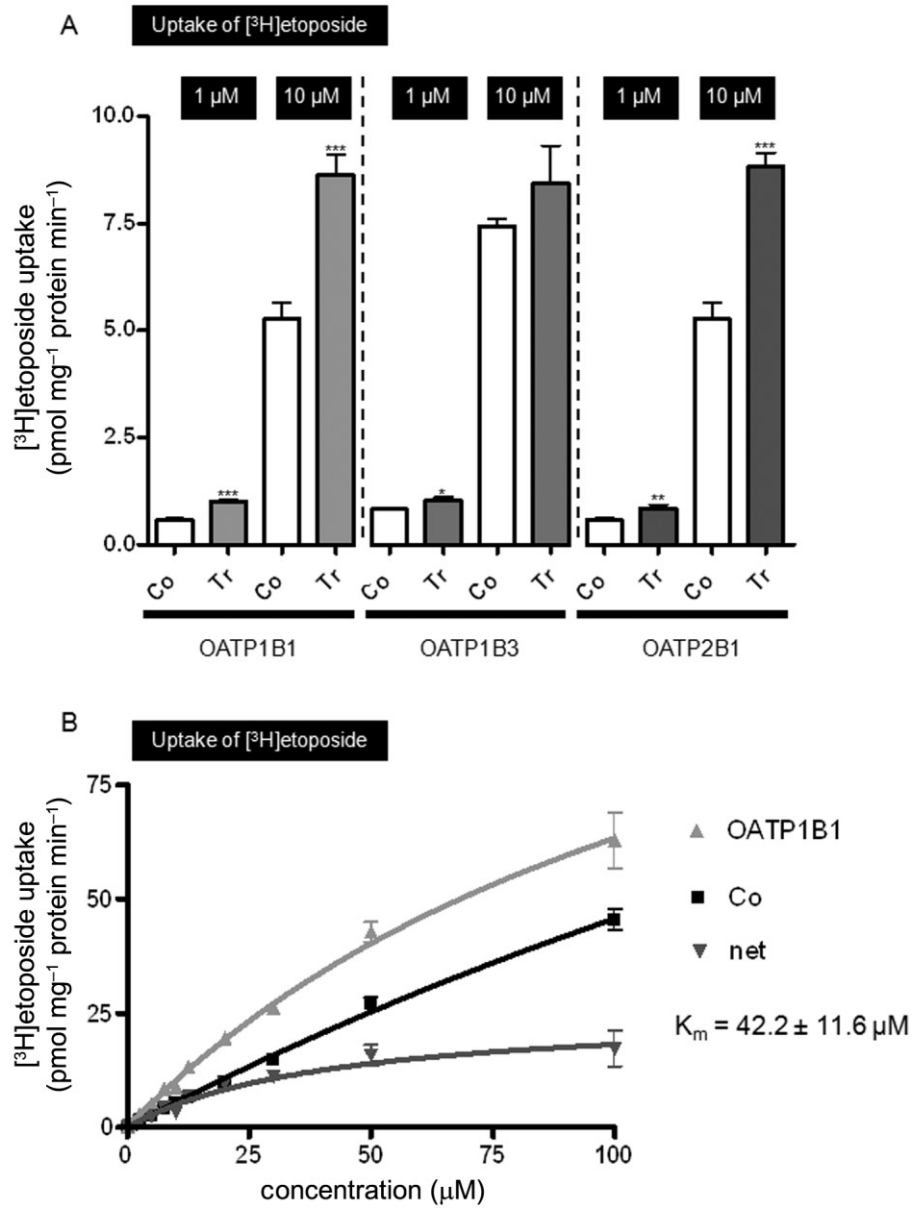

Figure 5

(A) Uptake of [^{3}H] etoposide (1 and 10 µM; 5 min) into HEK-OATP1B1 (OATP1B1), HEK-OATP1B3 (OATP1B3) and HEK-OATP2B1 (OATP2B1) and respective control cells (Co). (B) Concentration-dependent uptake of [^{3}H] etoposide (5 min) into HEK-OATP1B1 (OATP1B1) and respective control cells (Co). Net uptake was calculated by subtracting the uptake values from the control cells from the respective uptake values in the HEK-OATP1B1 cells. *P < 0.05, **P < 0.01, ***P < 0.001 versus control cells (unpaired t-test). Tr, stably transfected cell line.

indicating that UGT1A1 is involved in ezetimibe glucuronidation. Two studies have shown that the ATP-dependent transport of 17β-glucuronosyl oestradiol into isolated MRP2-containing inside-out vesicles was inhibited by ezetimibe glucuronide (Oswald *et al.*, 2006a; de Waart *et al.*, 2009). However, whether ezetimibe glucuronide is also a substrate of human MRP2 was not investigated. Additional data on the impact of MRP2/Mrp2 on the disposition of ezetimibe glucuronide are available from studies in rodents with lacking Mrp2 expression. First, serum concentrations of ezetimibe glucuronide were considerably increased in Mrp2-deficient rats compared with wild-type animals (Oswald *et al.*, 2008; 2010). Second, Mrp2-deficient mice accumulated significantly more ezetimibe glucuronide in the liver and eliminated less ezetimibe glucuronide into bile compared to Mrp2-expressing animals (de Waart *et al.*, 2009). It should be noted that the data from de Waart *et al.* (2009) indicate that other rodent efflux transporters (Bcrp, Mrp3) also have an impact on intestinal, portal venous or biliary concentrations of ezetimibe glucuronide. Further studies are needed to clarify whether human BCRP or MRP3 are capable of transporting ezetimibe glucuronide.

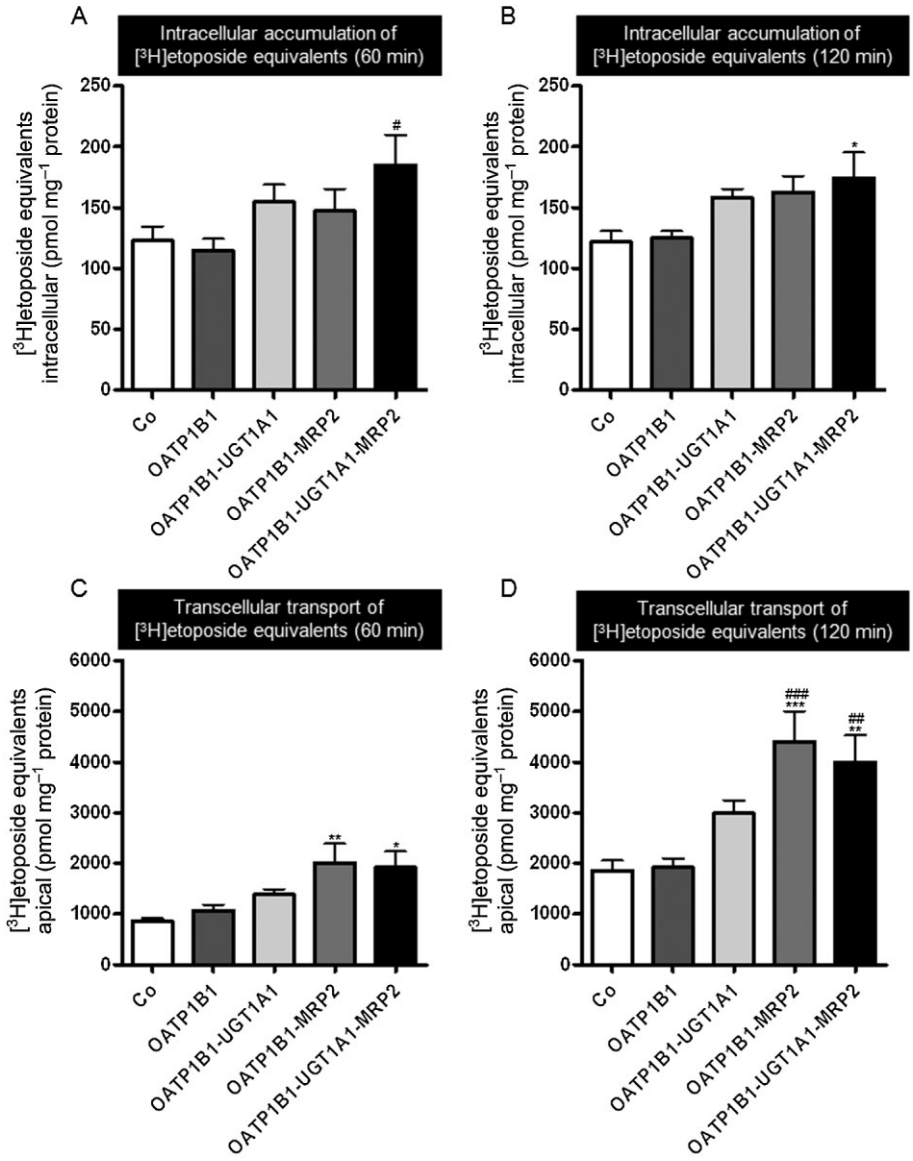

Figure 6

[^{3}H] Etoposide (10 μM) was administered to the basal side of monolayers of MDCK-control (Co), single- (OATP1B1), double- (OATP1B1-UGT1A1, OATP1B1-MRP2) and triple-transfected cells (OATP1B1-UGT1A1-MRP2). Intracellular accumulation of etoposide equivalents (i.e. parent compound and metabolites) in the cells (A, B) and translocation of etoposide equivalents into the apical compartment after 60 min and 120 min (C, D) are shown. Data are shown as mean value ± SD.*$P < 0.05$, **$P < 0.01$, ***$P < 0.001$ versus MDCK-Co; $^{\#}P < 0.05$, $^{\#\#}P < 0.01$, $^{\#\#\#}P < 0.001$ versus MDCK-OATP1B1 cells.

In addition to ezetimibe, we used our triple-transfected MDCK-OATP1B1-UGT1A1-MRP2 cell line to investigate the impact of these three proteins on polarized transport of another clinically important drug, etoposide, which also interacts with OATP1B1 (results of this study) and UGT1A1 (Watanabe *et al.*, 2003; Wen *et al.*, 2007). Glucuronide conjugates of etoposide have been detected in urine and bile (for review, see Clark and Slevin, 1987). Using HEK cells expressing the three hepatic OATPs, we showed for the first time that etoposide is a substrate of OATP1B1 and OATP2B1, and if at all, only a poor substrate of OATP1B3, with a K_m value for OATP1B1-mediated etoposide transport of 42.2 μM. The clinical relevance of this finding, which also relates to the role of *SLCO1B1* polymorphisms affecting drug disposition, beneficial effects and side effects (Fahrmayr *et al.*, 2010; König, 2011), remains to be studied. Since etoposide can also be administered orally, particularly high concentrations can be expected in portal venous blood and at the transporter located in the basolateral membrane of hepatocytes after oral administration of the drug. In contrast to the result with the HEK-OATP1B1 cells, intracellular accumulation of etoposide was not significantly different from control cells when MDCK-OATP1B1 cell monolayers were used. We speculate that OATP1B1-mediated etoposide uptake is reversed by back

extrusion into the basal compartment due to endogenous export transporters [e.g. MRP3 (Zelcer *et al.*, 2001)] located in the basolateral membrane of the MDCK cells. The data from the apical accumulation of etoposide equivalents indicate that etoposide and possibly also its glucuronide are substrates of MRP2. Accumulation of etoposide equivalents in the apical compartment after 120 min was 115% higher in MDCK-OATP1B1-UGT1A1-MRP2 cells, compared with control cells. Interestingly, the presence of the uptake and the efflux transporters without UGT1A1 (MDCK-OATP1B1-MRP2) led to a similar accumulation of etoposide equivalents in the apical compartment (+137%) as in the monolayers of the triple-transfected cells. One reason could be that etoposide and etoposide glucuronide show a competitive interaction for MRP2-mediated export, which would result in similar transport rates as observed in the MDCK-OATP1B1-MRP2 cells. Further studies are needed to analyse the relative amounts of etoposide and its glucuronide in the apical compartment. Our findings are in line with previous studies indicating that etoposide is a substrate of human MRP2 (Cui *et al.*, 1999; Guo *et al.*, 2002; Huisman *et al.*, 2005). Results from the recent study by Lagas *et al.* (2010) indicate that etoposide and its glucuronide are substrates of mouse Mrp2 with additional contributions of mouse P-glycoprotein and Mrp3 to the disposition of etoposide and its glucuronide *in vivo*.

Taken together, polarized cell lines simultaneously expressing human hepatic uptake transporters, drug-metabolizing enzymes and efflux transporters can contribute together with data from primary hepatocytes, animal models and clinical studies to an improved understanding of the hepatic disposition of frequently used drugs.

Acknowledgements

We thank C. Hoffmann, K. Singer and E. Hoier for excellent technical assistance. This work was supported by the DOKTOR ROBERT PFLEGER-STIFTUNG Bamberg and in part by the Deutsche Forschungsgemeinschaft (Fr 1298/5-1).

Conflict of interest

None.

References

Altmann SW, Davis HR Jr, Zhu LJ, Yao X, Hoos LM, Tetzloff G *et al.* (2004). Niemann-Pick C1 Like 1 protein is critical for intestinal cholesterol absorption. Science 303: 1201–1204.

Cai H, Nguyen N, Peterkin V, Yang YS, Hotz K, La Placa DB *et al.* (2010). A humanized UGT1 mouse model expressing the UGT1A1*28 allele for assessing drug clearance by UGT1A1-dependent glucuronidation. Drug Metab Dispos 38: 879–886.

Clark PI, Slevin ML (1987). The clinical pharmacology of etoposide and teniposide. Clin Pharmacokinet 12: 223–252.

Cui Y, König J, Buchholz JK, Spring H, Leier I, Keppler D (1999). Drug resistance and ATP-dependent conjugate transport mediated by the apical multidrug resistance protein, MRP2, permanently expressed in human and canine cells. Mol Pharmacol 55: 929–937.

Cui Y, König J, Keppler D (2001). Vectorial transport by double-transfected cells expressing the human uptake transporter SLC21A8 and the apical export pump ABCC2. Mol Pharmacol 60: 934–943.

Fahrmayr C, Fromm MF, König J (2010). Hepatic OATP and OCT uptake transporters: their role for drug-drug interactions and pharmacogenetic aspects. Drug Metab Rev 42: 380–401.

Fehrenbach T, Cui Y, Faulstich H, Keppler D (2003). Characterization of the transport of the bicyclic peptide phalloidin by human hepatic transport proteins. Naunyn Schmiedebergs Arch Pharmacol 368: 415–420.

Funk C (2008). The role of hepatic transporters in drug elimination. Expert Opin Drug Metab Toxicol 4: 363–379.

Ghosal A, Hapangama N, Yuan Y, Achanfuo-Yeboah J, Iannucci R, Chowdhury S *et al.* (2004). Identification of human UDP-glucuronosyltransferase enzyme(s) responsible for the glucuronidation of ezetimibe (Zetia). Drug Metab Dispos 32: 314–320.

Guo A, Marinaro W, Hu P, Sinko PJ (2002). Delineating the contribution of secretory transporters in the efflux of etoposide using Madin-Darby canine kidney (MDCK) cells overexpressing P-glycoprotein (Pgp), multidrug resistance-associated protein (MRP1), and canalicular multispecific organic anion transporter (cMOAT). Drug Metab Dispos 30: 457–463.

Huisman MT, Chhatta AA, van Tellingen O, Beijnen JH, Schinkel AH (2005). MRP2 (ABCC2) transports taxanes and confers paclitaxel resistance and both processes are stimulated by probenecid. Int J Cancer 116: 824–829.

Jedlitschky G, Leier I, Buchholz U, Hummel-Eisenbeiss J, Burchell B, Keppler D (1997). ATP-dependent transport of bilirubin glucuronides by the multidrug resistance protein MRP1 and its hepatocyte canalicular isoform MRP2. Biochem J 327: 305–310.

Keppler D, Kartenbeck J (1996). The canalicular conjugate export pump encoded by the cMRP/cMOAT gene. Prog Liver Dis 14: 55–67.

Kindla J, Müller F, Mieth M, Fromm MF, König J (2011). Influence of non-steroidal anti-inflammatory drugs (NSAIDs) on OATP1B1- and OATP1B3-mediated drug transport. Drug Metab Dispos 39: 1047–1053.

König J (2011). Uptake transporters of the human OATP family: molecular characteristics, substrates, their role in drug-drug interactions, and functional consequences of polymorphisms. In: Fromm MF and Kim RB (eds). Drug Transporters. Handbook of Experimental Pharmacology 201, Vol. 201. Springer-Verlag: Berlin Heidelberg, pp. 1–28.

König J, Rost D, Cui Y, Keppler D (1999). Characterization of the human multidrug resistance protein isoform MRP3 localized to the basolateral hepatocyte membrane. Hepatology 29: 1156–1163.

König J, Cui Y, Nies AT, Keppler D (2000). A novel human organic anion transporting polypeptide localized to the basolateral hepatocyte membrane. Am J Physiol Gastrointest Liver Physiol 278: G156–G164.

König J, Zolk O, Singer K, Hoffmann C, Fromm MF (2010). Double-transfected MDCK cells expressing human OCT1/MATE1 or OCT2/MATE1: determinants of uptake and transcellular translocation of organic cations. Br J Pharmacol 163: 546–555.

Kopplow K, Letschert K, König J, Walter B, Keppler D (2005). Human hepatobiliary transport of organic anions analyzed by quadruple-transfected cells. Mol Pharmacol 68: 1031–1038.

Kosoglou T, Statkevich P, Johnson-Levonas AO, Paolini JF, Bergman AJ, Alton KB (2005). Ezetimibe: a review of its metabolism, pharmacokinetics and drug interactions. Clin Pharmacokinet 44: 467–494.

Lagas JS, Fan L, Wagenaar E, Vlaming ML, van Tellingen O, Beijnen JH *et al*. (2010). P-glycoprotein (P-gp/Abcb1), Abcc2, and Abcc3 determine the pharmacokinetics of etoposide. Clin Cancer Res 16: 130–140.

Mandery K, Bujok K, Schmidt I, Wex T, Treiber G, Malfertheiner P *et al*. (2009). Influence of cyclooxygenase inhibitors on the function of the prostaglandin transporter organic anion-transporting polypeptide 2A1 expressed in human gastroduodenal mucosa. J Pharmacol Exp Ther 332: 345–351.

Ng KH, Lim BG, Wong KP (2003). Sulfate conjugating and transport functions of MDCK distal tubular cells. Kidney Int 63: 976–986.

Nies AT, Herrmann E, Brom M, Keppler D (2008). Vectorial transport of the plant alkaloid berberine by double-transfected cells expressing the human organic cation transporter 1 (OCT1, SLC22A1) and the efflux pump MDR1 P-glycoprotein (ABCB1). Naunyn Schmiedebergs Arch Pharmacol 376: 449–461.

Oswald S, Haenisch S, Fricke C, Sudhop T, Remmler C, Giessmann T *et al*. (2006a). Intestinal expression of P-glycoprotein (ABCB1), multidrug resistance associated protein 2 (ABCC2), and uridine diphosphate-glucuronosyltransferase 1A1 predicts the disposition and modulates the effects of the cholesterol absorption inhibitor ezetimibe in humans. Clin Pharmacol Ther 79: 206–217.

Oswald S, Scheuch E, Cascorbi I, Siegmund W (2006b). A LC-MS/MS method to quantify the novel cholesterol lowering drug ezetimibe in human serum, urine and feces in healthy subjects genotyped for SLCO1B1. J Chromatogr B Analyt Technol Biomed Life Sci 830: 143–150.

Oswald S, König J, Lütjohann D, Giessmann T, Kroemer HK, Rimmbach C *et al*. (2008). Disposition of ezetimibe is influenced by polymorphisms of the hepatic uptake carrier OATP1B1. Pharmacogenet Genomics 18: 559–568.

Oswald S, May K, Rosin J, Lütjohann D, Siegmund W (2010). Synergistic influence of Abcb1 and Abcc2 on disposition and sterol lowering effects of ezetimibe in rats. J Pharm Sci 99: 422–429.

Oswald S, Nassif A, Modess C, Keiser M, Ulrich A, Runge D *et al*. (2011). Drug interactions between the immunosuppressant tacrolimus and the cholesterol absorption inhibitor ezetimibe in healthy volunteers. Clin Pharmacol Ther 89: 524–528.

Patrick JE, Kosoglou T, Stauber KL, Alton KB, Maxwell SE, Zhu Y *et al*. (2002). Disposition of the selective cholesterol absorption inhibitor ezetimibe in healthy male subjects. Drug Metab Dispos 30: 430–437.

Sato T, Masuda S, Yonezawa A, Tanihara Y, Katsura T, Inui K (2008). Transcellular transport of organic cations in double-transfected MDCK cells expressing human organic cation transporters hOCT1/hMATE1 and hOCT2/hMATE1. Biochem Pharmacol 76: 894–903.

Seithel A, Eberl S, Singer K, Auge D, Heinkele G, Wolf NB *et al*. (2007). The influence of macrolide antibiotics on the uptake of organic anions and drugs mediated by OATP1B1 and OATP1B3. Drug Metab Dispos 35: 779–786.

de Waart DR, Vlaming ML, Kunne C, Schinkel AH, Oude Elferink RP (2009). Complex pharmacokinetic behavior of ezetimibe depends on abcc2, abcc3, and abcg2. Drug Metab Dispos 37: 1698–1702.

Watanabe Y, Nakajima M, Ohashi N, Kume T, Yokoi T (2003). Glucuronidation of etoposide in human liver microsomes is specifically catalyzed by UDP-glucuronosyltransferase 1A1. Drug Metab Dispos 31: 589–595.

Wen Z, Tallman MN, Ali SY, Smith PC (2007). UDP-glucuronosyltransferase 1A1 is the principal enzyme responsible for etoposide glucuronidation in human liver and intestinal microsomes: structural characterization of phenolic and alcoholic glucuronides of etoposide and estimation of enzyme kinetics. Drug Metab Dispos 35: 371–380.

Zelcer N, Saeki T, Reid G, Beijnen JH, Borst P (2001). Characterization of drug transport by the human multidrug resistance protein 3 (ABCC3). J Biol Chem 276: 46400–46407.

Zolk O, Fromm MF (2011). Transporter-mediated drug uptake and efflux: important determinants of adverse drug reactions. Clin Pharmacol Ther 89: 798–805.

Supporting information

Additional Supporting Information may be found in the online version of this article:

Figure S1 Chemical structures of ezetimibe and etoposide. Radiolabelled compounds were generally labelled.

Please note: Wiley-Blackwell are not responsible for the content or functionality of any supporting materials supplied by the authors. Any queries (other than missing material) should be directed to the corresponding author for the article.